J|A|C|S COMMUNICATIONS

Published on Web 04/05/2010

Plasmon-Enhanced Fluorescence from Single Fluorophores End-Linked to Gold Nanorods

Yi Fu,* Jian Zhang, and Joseph R. Lakowicz

University of Maryland School of Medicine, 725 West Lombard Street, Baltimore, Maryland 21201

Received November 12, 2009; E-mail: yifu@cfs.biomet.umaryland.edu

Current biological studies are limited by existing fluorescent probes which suffer from intrinsic deficits, particularly poor photostability and low emission intensities, restraining their applications in dynamics studies.[1] It is crucial to create a versatile set of probes with improved photostability and higher emission rates to advance studies of individual biomolecule function.

We now know that strong resonant coupling between the excitation light and the noble metal nanoparticles leads to a number of remarkable optical effects, including a considerable near-field enhancement of fluorescence at the metal surface.[2−4] It suggests that the optical absorption and scattering properties of metallic nanostructures can be used to control the radiative decay rate and direction of fluorophore emission. Enhancement and quenching of fluorescence by noble metal nanoparticles have been reported mainly for spheres, aggregates, and nanoshells.[5−11] Using the elongated resonance shape and fluorophore distance from the metal surface, the fluorescence can be significantly modified.[12] We report here the use of single gold nanorods as metallic plasmonic structures. Through covalent linkages of fluorophores at the preferred longitudinal axis of the nanorods, we are able to increase the overall optical signal for improved sensitivity. These effects may be used for increased detectability of single molecules bound to surfaces which contain metallic structures in a nonrandom fashion, for either biophysical studies or high sensitivity assays.

We synthesized gold nanorods in aqueous solution using a seed-mediated route in the presence of cetyltrimethylammonium bromide (CTAB).[13] After synthesis, the colloidal suspensions were repeatedly centrifuged and washed with deionized water to remove excess surfactant. The average aspect ratio of the rods was 6 (ca. 80 nm in length and 13 nm in diameter) as inferred from transmission electron microscopy (TEM) and the longitudinal plasmon band at 980 nm (Supporting Information). Functionalization of the nanorods was performed according to the reported method.[14] Owing to the preferred binding of thiol molecules to the gold nanorod edges rather than the side faces,[14,15] the biotin-capped gold rod ends were achieved, which led to the end linkage upon subsequent addition of streptavidin (Scheme 1). Aggregation of end-to-end linked Au nanorods was minimized under the selected concentrations. The functionalized nanorods were incubated with a low concentration solution of oligonucleotides labeled with biotin and Cy5 (Biotin-3′-AGG-TGT-ATG-ACC-GGT-AGA-AG-5′-Cy5, ca. 8 nm in length) to obtain the hybrid nanocomplexes (Supporting Information).

Figure 1 shows typical 10 μm × 10 μm confocal scanning images taken from the individual Cy5-tagged ssDNA (a) and nanocomposites (b) deposited on glass coverslips, respectively. The noticeable differences in brightness of emission spots indicate preliminary information of enhanced fluorescence emission in the presence of gold nanostructures. Panel c in Figure 1 illustrates a time trace of a single dye-labeled ssDNA suffered photobleaching as evidenced by the discrete drop in fluorescence intensity to the background

Scheme 1. Conjugation of a Dye Labeled Single Stranded DNA to a Biotin End-Capped Gold Nanorod

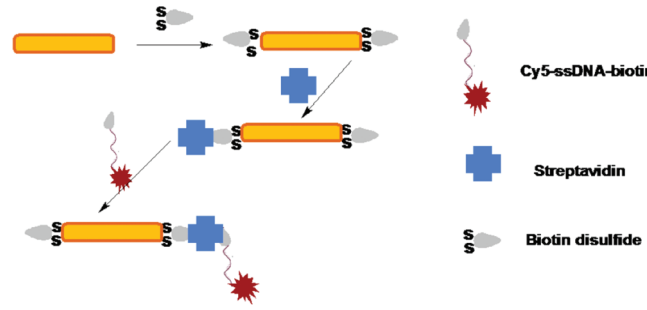

level. Most of the spots investigated suffered permanent photobleaching in an abrupt step, ensuring a single binding event had been observed. Panel d in Figure 1 depicts a typical time trace observed from Au/ssDNA hybrid nanocomplexes. In contrast, a

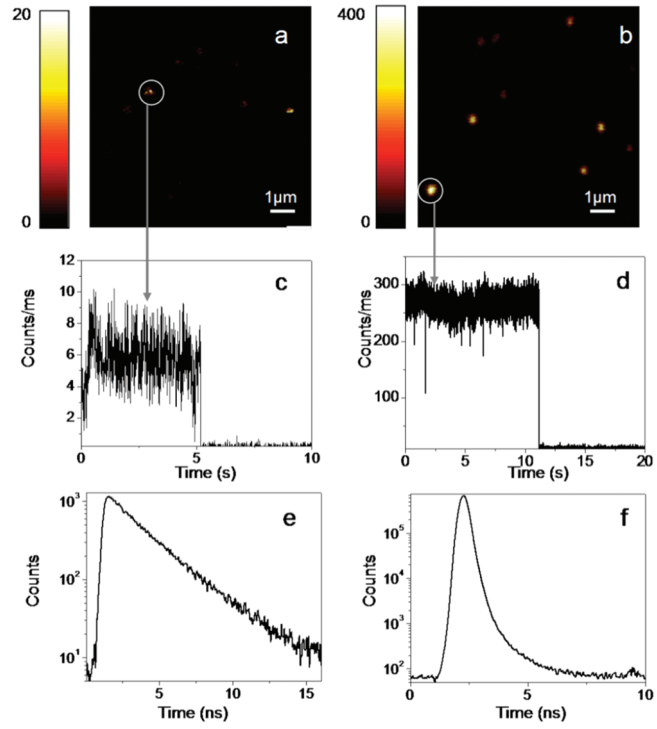

Figure 1. (a) A confocal scanning fluorescence image of Cy5-ss-DNA deposited on glass coverslip. (b) A scanning fluorescence image of Au/Cy5-ssDNA adsorbed on APS-modified glass coverslip. (c) Fluorescence time trace of Cy5 shown in Figure 1a. (d) Fluorescence time trace of Au/Cy5 shown in Figure 1b. (e) Fluorescence decay of Cy5 derived from Figure 1c. (f) Fluorescence decay of Au/Cy5 derived from Figure 1d. Excitation intensity: 100 nW. Excitation wavelength: 633 nm. Emission was collected through a 685/35 band-pass filter (Supporting Information).

10.1021/ja9096237

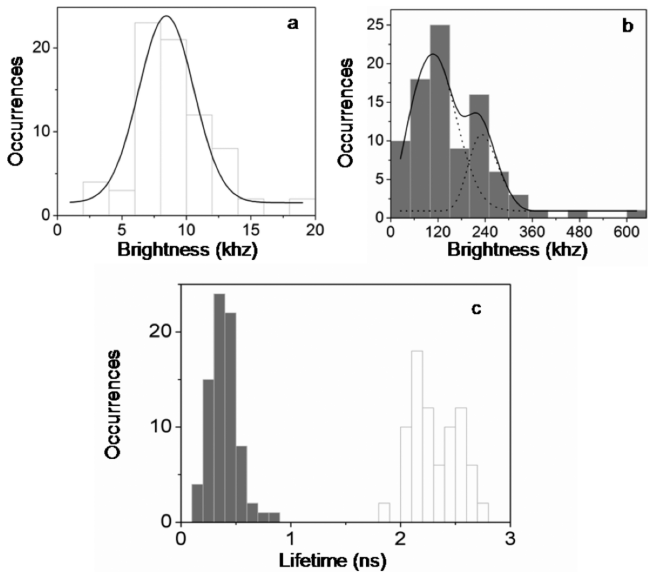

Figure 2. (a) Brightness histogram of free Cy5-ssDNA on glass coverslips. (b) Brightness histogram of single Au nanocomplexes on glass coverslips. (c) Lifetime histograms of single molecules. White bars: free Cy5-ssDNA; gray bars: Au nanocomplexes.

much higher emission rate is clearly observed, which is approximately 40-fold greater than that observed in the absence of gold nanostructure. We occasionally noticed two-step or multiple-step photobleaching behaviors (Supporting Information), showing a possibility that two or more molecules were present under the focusing volume, indicating two or more biotin-ssDNA molecules conjugated to the streptavidin end-capped nanorods. Despite the fact, the overall enhancement in fluorescence intensity was observed for the fluorophores located at the ends of nanorods.

The single molecule fluorescence lifetime measurement is implemented using time-correlated single photon counting by plotting a histogram of time lags between the excitation pulses and the detected fluorescence photons. The analysis of the fluorescence signal of Cy5-ssDNA on glass (panel d in Figure 1) yields an averaged lifetime $\tau = 2.51$ ns. In contrast, we observed a considerable decrease in the lifetime of single Au nanocomplexes (panel f in Figure 1, $\tau = 0.33$ ns). Clearly, the fluorescence decay of the Au nanocomplexes is faster than that of the free probe on glass. This suggests that the fluorescence decay rate of the fluorophore is substantially affected by the Au nanorod.

Figure 2 illustrates brightness histograms acquired from ~80 single molecules of Cy5-ssDNA and Au nanocomplexes, respectively. To aid interpretation, brightness distributions were fit to Gaussian functions. A symmetric distribution with a mean value equal to 8 counts/ms is obtained for dye molecules immobilized on bare glass coverslips, indicating the free probe sample is relatively homogeneous. The brightness of the Au hybrid nanocomplexes is shifted well to the much higher values as shown in Figure 2b. In contrast to the symmetric distribution shown in Figure 2a, the brightness distribution is much broader, depicting the likely existence of two different subpopulations of single molecule species arising from diverse near-field electromagnetic interactions. The end-linked dye probes randomly oriented along the longitudinal axis of the nanorods and led to variation of fluorescence enhancements. According to the radiating plasmons (RPs) model, the relatively larger elongated gold nanorods display a dominant scattering component over an absorption component above 600 nm and are expected to enhance the fluorescence of fluorophores emitting at wavelengths longer than 600 nm.[7,16,17] Additionally, we observed the polarization dependence of the excitation, which was demonstrated on a single Au nanocomplex excited at different directions (Supporting Information). The emission intensity dropped abruptly as the excitation angle rotated 90°, indicating that the magnitude of the enhancement depends on the location of the fluorophore around the particle and the orientation of its dipole moment relative to the metallic surface.

The lifetime histograms of Cy5-ssDNA in the presence and in the absence of Au nanorods illustrate roughly symmetric distributions in two distinct ranges, respectively. Significantly shortened lifetimes of Au nanocomplexes confirm the increased radiative decay rate of the fluorophores in the presence of a metallic nanoobjective. An increase in the radiative decay rate results in an increased intensity (due to the increased quantum yield) and reduced lifetime.[17]

In summary, we observed a remarkable increase in fluorescence of single fluorophores controllably linked to ends of Au nanorods. The fluorescence enhancement to a nanorod end-linked fluorophore is due to a combination of processes including the local electric field intensity contour around the nanorods, modification of the radiative decay rate, and the local orientations of dye molecules. The result suggests a facile approach to controllably fabricate nanometer-scale probes, which is useful for single molecule imaging applications.

Acknowledgment. This work was supported by the NHGRI (HG002655) and NIBIB (EB006521 and EB009509).

Supporting Information Available: Experimental details, TEM images, time traces, fluorescence intensity images under polarized excitation lights. Further details are given as noted in the text. This material is available free of charge via the Internet at http://pubs.acs.org.

References

(1) Mehta, A. D.; Rief, M.; Spudich, J. A. *J. Biol. Chem.* **1999**, *274*, 14517.
(2) Lakowicz, J. R.; Ray, K.; Chowdhury, M.; Szmacinski, H.; Fu, Y.; Zhang, J.; Nowaczyk, K. *Analyst* **2008**, *133*, 1308.
(3) Bharadwaj, P.; Anger, P.; Novotny, L. *Nanotechnology* **2007**, 18.
(4) Liebermann, T.; Knoll, W. *Colloids Surf.* **2000**, *171*, 115.
(5) Bakker, R. M.; Drachev, V. P.; Liu, Z. T.; Yuan, H. K.; Pedersen, R. H.; Boltasseva, A.; Chen, J. J.; Irudayaraj, J.; Kildishev, A. V.; Shalaev, V. M. *New J. Phys.* **2008**, 10.
(6) Bakker, R. M.; Yuan, H. K.; Liu, Z. T.; Drachev, V. P.; Kildishev, A. V.; Shalaev, V. M.; Pedersen, R. H.; Gresillon, S.; Boltasseva, A. *Appl. Phys. Lett.* **2008**, *92*, 043101.
(7) Bardhan, R.; Nathaniel K, G.; Cole, J. R.; Joshi, A.; Halas, N. J. *ACS Nano* **2009**, *3*, 744.
(8) Bek, A.; Jansen, R.; Ringler, M.; Mayilo, S.; Klar, T. A.; Feldmann, J. *Nano Lett.* **2008**, *8*, 485.
(9) Haldar, K. K.; Patra, A. *Appl. Phys. Lett.* **2009**, 95.
(10) Hossain, M. K.; Huang, G. G.; Kaneko, T.; Ozaki, Y. *Chem. Phys. Lett.* **2009**, *477*, 130.
(11) Tovmachenko, O. G.; Graf, C.; van den Heuvel, D. J.; van Blaaderen, A.; Gerritsen, H. C. *Adv. Mater.* **2006**, *18*, 91.
(12) Ming, T.; Zhao, L.; Yang, Z.; Chen, H.; Sun, L.; Wang, J.; Yan, C. *Nano Lett.* **2009**, *9*, 3896.
(13) Jana, N. R.; Gearheart, L.; Murphy, C. J. *J. Phys. Chem. B* **2001**, *105*, 4065.
(14) Caswell, K. K.; Wilson, J. N.; Bunz, U. H. F.; Murphy, C. J. *J. Am. Chem. Soc.* **2003**, *125*, 1391.
(15) Chang, J. Y.; Wu, H. M.; Chen, H.; Ling, Y. C.; Tan, W. H. *Chem. Commun.* **2005**, 1092.
(16) Lakowicz, J. R. *Anal. Biochem.* **2001**, *298*, 1.
(17) Lakowicz, J. R.; Malicka, J.; Gryczynski, I.; Gryczynski, Z.; Geddes, C. D. *J. Phys. D: Appl. Phys.* **2003**, *36*, R240.

JA9096237